Optical Spectroscopy of a Polyfluorene Copolymer at High Pressure: Intra- and Intermolecular Interactions

Johanna P. Schmidtke,[1,*] Ji-Seon Kim,[1] Johannes Gierschner,[2] Carlos Silva,[3] and Richard H. Friend[1]

[1]*Cavendish Laboratory, University of Cambridge, J. J. Thompson Avenue, Cambridge CB3 0HE, United Kingdom*

[2]*Laboratory for Chemistry of Novel Materials, Center for Research in Molecular Electronics and Photonics, University of Mons-Hainaut, Place du Parc 20, B-7000 Mons, Belgium*

[3]*Département de physique, Regroupement québécois sur les matériaux de pointe, Université de Montréal, C. P. 6128, Succ. centre-ville, Montréal, Québec H3C 3J7, Canada*

(Received 8 March 2007; published 19 October 2007)

We present optical spectroscopy studies of the conjugated polymer poly(9,9-di-*n*-octylfluorene-*alt*-benzothiadiazole) (F8BT) at high pressure. The photoluminescence spectrum of F8BT in a dilute solid-state solution in polystyrene redshifts by 320 meV over 7.4 GPa, while that of a F8BT thin film redshifts 460 meV over a comparable pressure range. We attribute the redshift in solution to intrachain pressure effects, principally conformational planarization. The additional contribution from interchain π-electron interactions accounts for the larger redshift of thin films.

DOI: 10.1103/PhysRevLett.99.167401 PACS numbers: 78.66.Qn, 78.40.Me, 78.55.−m

Since the first demonstration of electroluminescence in poly(*p*-phenylene vinylene) (PPV), conjugated polymers (CPs) have been widely investigated for optoelectronic applications [1–3]. Central to realizing the utility of such CPs in new applications is an understanding of their complex photophysics, which differ significantly from those of their inorganic counterparts. In particular, a clear description of intermolecular interactions in the solid state is critical to the understanding of charge transport, exciton migration, and defect emission in CPs [4–7]. In CP bulk-heterojunction devices, intermolecular states are central to the primary optoelectronic device processes—charge separation and recombination [8].

Studies often rely upon chemical modifications or modified processing conditions to vary the extent of intermolecular interactions in the material [4]. Applying hydrostatic pressure is a clean, simple method to probe intermolecular interactions of a single material for a range of intermolecular distances without such alterations. High-pressure x-ray diffraction studies of polythiophenes have demonstrated that pressures of 8.0 GPa result in a 5–15% reduction in intermolecular distance [9]. Previous high-pressure optical spectroscopy studies of CPs include work on PPV- [10] and polydiacetylene derivatives [11], poly(*p*-phenylene) and oligo(*p*-phenylenes) (OPPs) [12,13], polythiophenes and oligothiophenes [14,15], and polyfluorenes [16]. In these studies, both intra- and intermolecular effects have been described at high external pressures [12,13,15]. However, a clean separation of intra- and intermolecular effects has not been shown previously. We report high-pressure optical spectroscopy studies of the electron-accepting polyfluorene copolymer poly(9,9-di-*n*-octylfluorene-*alt*-benzothiadiazole) (F8BT). We unravel intra- and intermolecular interactions in F8BT as a function of external hydrostatic pressure.

All samples were prepared via spin casting from chloroform solutions onto spectrosil substrates in a nitrogen atmosphere. Thin film samples (approx. 50 μm $\times$ 50 μm area) for high-pressure measurements were cut from the spin-cast thin films using a razor blade. Hydrostatic pressures were generated in a mini-cryogenic diamond anvil cell (DAC, Diacell Ltd. UK) using cryogenically-loaded argon as the pressure medium. The pressure was calibrated by the ruby fluorescence scale. Raman spectra were collected using a Renishaw Raman spectrometer with an Olympus BH-2 microscope modified for high-pressure measurements and the 1.96 eV line of a HeNe laser as the excitation source. Steady-state and time-resolved photoluminescence (PL) spectra were determined by time-correlated single photon counting. The samples were excited with a pulsed diode laser [PicoQuant LDH400, 20 MHz, 70 ps full width at half-maximum, 3.05 eV]. The luminescence was detected with a microchannel plate photomultiplier (Hamamatsu) coupled to a monochromator and TCSPC electronics (Edinburgh Instruments Lifespec-ps and VTC900 PCI card). Temperature-dependent PL spectra were measured using an Optistat dynamic flow cryostat. Absorption spectra were determined via transmission through the pressure cell using monochromatic light from an Xe lamp as the excitation. The transmitted light was detected with a Si photodiode using a lockin technique.

In order to disentangle the intra- and intermolecular effects of hydrostatic pressure, we aimed to compare the pressure dependence of the PL of F8BT thin films to that of isolated F8BT chains within an inert matrix. However, 0.02% w/w blends of high molecular weight, M_n, F8BT in polystyrene (PS) demonstrated a PL pressure dependence similar to that of F8BT thin films (not shown). Recent single-molecule PL spectroscopy studies of F6BT and F8BT in inert matrices including PS have shown that intramolecular chain-chain self-interactions are sufficient to allow for low-energy emission from single polymer chains [17,18]. Therefore, a low M_n F8BT (M_n = 9 kDa)

with an average length of 6 repeat units was used to achieve a blend PS matrix in which self-interaction of isolated F8BT molecules was minimal. Optical characterization of different M_n F8BTs has demonstrated that the optical properties of F8BT thin films vary minimally within the M_n range studied here [19]. The blend PS matrix was cast from chloroform using a low M_n PS ($M_n = 13$ kDa) to ensure the solubility of F8BT within the PS. Atomic force microscopy images (not shown) of the blend PS matrix are comparable to PS films, suggesting that there is no F8BT aggregation within the matrix. In addition, the PL spectra of the blend PS matrix at 0.1 MPa are comparable to the ensemble spectra of single-molecule PL studies of short-chain F8BT [18]. Therefore, we consider that a solid-state solution of isolated F8BT chains has been reasonably achieved in the blend PS matrix.

Pressure-dependent, steady-state PL spectra of F8BT ($M_n = 9$ kDa) in a thin film and in solid-state solution are compared in Fig. 1 for pressures up to 7.7 GPa. In the solid-state solution, the average energy of the F8BT emission (E_{PL}) is redshifted with increasing pressure by ~320 meV over 7.4 GPa. Because the F8BT chains are well separated within the matrix, this redshift is attributed to intrachain, pressure-induced effects upon F8BT. We note that no corrections have been made for the refractive index changes of the PS matrix under pressure, which may induce an additional redshift. In comparison, the E_{PL} of the thin film is redshifted by ~460 meV at a comparable pressure as seen in Fig. 1(b). The additional 140 meV redshift of the thin film PL spectrum indicates that hydrostatic pressure induces both intra- and intermolecular effects in the F8BT thin film.

Figure 2(a) presents pressure-dependent Raman spectra of F8BT in the region of the main two modes associated with the conjugated backbone—the ring-stretching modes of the polyfluorene (F8: 1608 cm^{-1} at 0.1 MPa) and benzothiadiazole (BT: 1545 cm^{-1} at 0.1 MPa) subunits [20,21]—for pressures of 0.1 MPa–1.8 GPa. It is evident that the relative intensity of the 1545 cm^{-1} mode compared to the 1608 cm^{-1} mode increases with pressure. In addition, a hardening and broadening of both modes is seen with increasing pressure. We note that due to the redshifted PL emission background, Raman spectra for pressures above 2 GPa were not obtained.

Reports on OPPs and PPV have correlated the relative intensities of two intramolecular Raman modes with the degree of planarization of the torsional angle between the aromatic rings of the conjugated backbone [12,22,23]. The influence of the F8-BT torsional angle, θ, upon the electronic properties and Raman spectra of a F8-BT-F8 unit were modeled in the gas phase by semi-empirical quantum chemical calculations at the INDO/SCI (intermediate neglect of differential overlap/singles-configuration interaction) level, as parameterized by Zerner and co-workers [24]. First, the ground-state geometries for a F8-BT-F8 unit with a range of torsional angles ($\theta = 0$–$90°$) were optimized under this constraint. Then, the wave functions

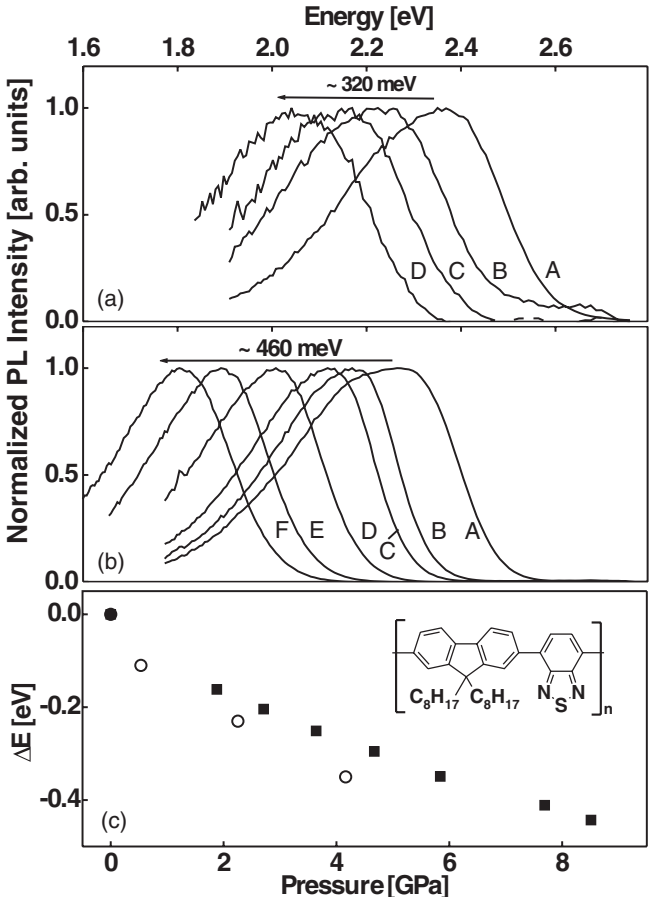

FIG. 1. Pressure-dependent, steady-state PL spectra of F8BT ($M_n = 9$ kDa) (a) in a solid-state solution (0.02% w/w in PS) for pressures of A: 0.1 MPa, B: 2.8 GPa, C: 4.5 GPa, and D: 7.4 GPa; and (b) as a thin film for pressures of A: 0.1 MPa, B: 1.2 GPa, C: 2.0 GPa, D: 3.8 GPa, E: 6.0 GPa, and F: 7.7 GPa. All spectra were measured using an excitation energy of 3.05 eV. (c) The change in E_{PL} (filled squares) and E_{Abs} (open circles) as a function of pressure for a F8BT ($M_n = 112$ kDa) thin film. Inset of (c) shows the chemical structure of F8BT.

of the highest occupied molecular orbital (HOMO) and lowest unoccupied molecular orbital (LUMO) were calculated for each conformation. Illustrations of the HOMO and LUMO topologies of a F8-BT-F8 unit in the lowest energy conformation with $\theta = 0°$ and $\theta = 90°$ are depicted in Fig. 2(c). For both the $\theta = 0°$ and $\theta = 90°$ conformations, the LUMO is localized on the BT unit. The HOMO is also localized in the $\theta = 90°$ conformation, having electronic density exclusively on the F8 units. However, in the $\theta = 0°$ conformation, the HOMO is delocalized across the F8-BT-F8 unit.

Raman spectra of a F8-BT-F8 unit were calculated by density functional theory (DFT) at the B3LYP/6-31G* level of theory within the GAUSSIAN98 package [25] for the optimized structures at $\theta = 0°$ and $\theta = 35°$, where the latter represents the most stable conformation at this level of theory. The calculated Raman spectra for the optimized structures with $\theta = 0°$ and $\theta = 35°$ are shown in Fig. 2(b)

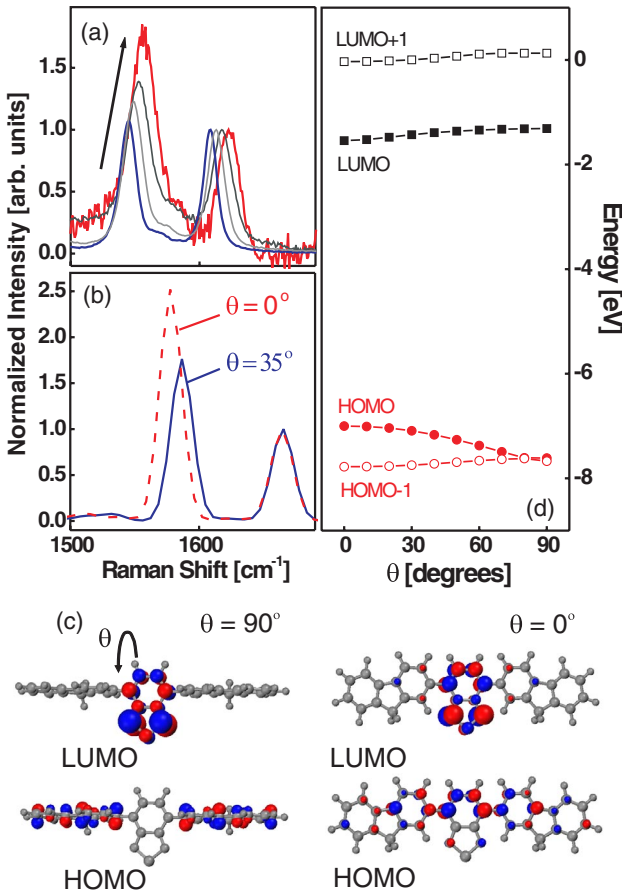

FIG. 2 (color online). (a) Raman spectra of F8BT (M_n = 9 kDa) in the region of the F8 (1608 cm^{-1} at 0.1 MPa) and BT (1545 cm^{-1} at 0.1 MPa) ring-stretching modes at pressures of 0.1 MPa–1.8 GPa (arrow indicates increasing pressure). The spectra are normalized to the intensity of the F8 ring-stretching mode. (b) DFT calculated Raman modes (normalized to the F8 ring-stretching mode) for a F8-BT-F8 unit with $\theta = 35°$ and $\theta = 0°$. (c) Illustration of the HOMO and LUMO topologies of a F8-BT-F8 unit with $\theta = 90°$ and $\theta = 0°$. (d) The calculated energy of the HOMO − 1, HOMO, LUMO, and LUMO + 1 of a F8-BT-F8 unit as a function of θ.

(normalized to the F8 mode intensity). The relative intensity of the 1545 cm^{-1} mode compared to the 1608 cm^{-1} mode in the calculated spectra correlates well to that observed in the high-pressure experiment [Fig. 2(a)]. The increased intensity of the 1545 cm^{-1} mode in the $\theta = 0°$ conformation is due to an increased coupling of the BT ring-stretching mode to the electronic HOMO-LUMO transition in the planar structure. These results indicate that the pressure-dependent variation in the relative Raman intensities observed for the 1545 cm^{-1} and 1608 cm^{-1} modes may be attributed to a decrease in the intramolecular F8-BT torsional angle, θ. The frequency shift and broadening of the intramolecular Raman modes observed experimentally at high pressure [Fig. 2(a)] are widely observed for conjugated materials and are attributed to an increased force constant of the covalent bonds with pressure [10,16,26].

The energetic consequences of a conformational planarization in F8BT are seen in Fig. 2(d), which depicts the calculated energy levels of the HOMO − 1, HOMO, LUMO, and LUMO + 1 for a range of θ. For smaller θ, a smaller HOMO-LUMO band gap is predicted due largely to the increased energy of the HOMO level. The predicted reduction in the band gap correlates with the experimental results in Fig. 1(c), in which a decreased energy of the absorption edge (E_{Abs}) of a F8BT (M_n = 112 kDa) thin film is observed with increasing pressure [27]. The redshift of E_{Abs} is of similar magnitude of the shift in E_{PL} in thin films, but by definition may overestimate the redshift of the average energy of absorption. In addition, from the illustrations of the HOMO and LUMO topologies shown in Fig. 2(c), it is evident that there is greater overlap between the LUMO and delocalized HOMO in the $\theta = 0°$ structure than in the $\theta = 90°$ structure. As a result, a larger oscillator strength is expected in more planar conformations. Between 0.5–4.5 GPa, a factor of 2 increase in oscillator strength was observed in optical absorption spectra of F8BT thin films at high pressures. Finally, the large decrease in the HOMO-LUMO band gap predicted by these calculations qualitatively correlates with the pressure-dependent redshift of the PL spectra of the dilute solid-state solution of F8BT in Fig. 1(a).

In Fig. 3, time-resolved PL spectra of a solid-state solution of F8BT (M_n = 9 kDa) at pressures of 0.1 MPa and 5.0 ± 0.4 GPa and a F8BT (M_n = 9 kDa) thin film at pressures of 0.1 MPa and 6.0 ± 0.2 GPa are presented for time delays of 0.6–15 ns. Under external pressure, a larger

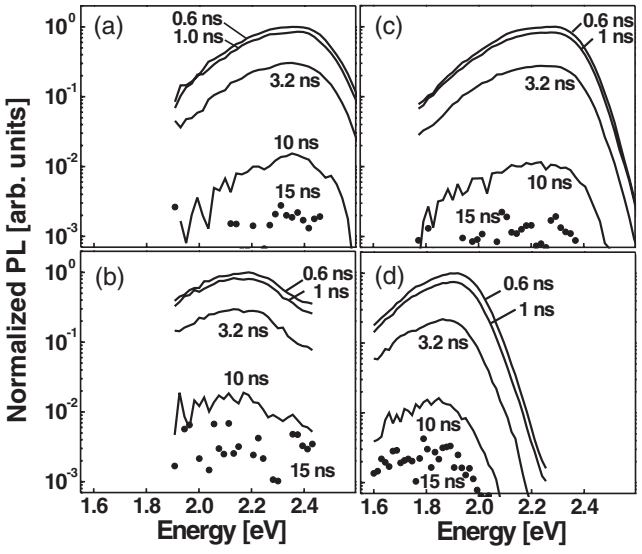

FIG. 3. Normalized time-resolved PL spectra of F8BT (M_n = 9 kDa) in a solid-state solution (0.02% w/w in PS) at pressures of (a) 0.1 MPa and (b) 5.0 ± 0.4 GPa; and as a thin film at (c) 0.1 MPa and (d) 6.0 ± 0.2 GPa. The time delay after excitation for each spectra is shown in the figure.

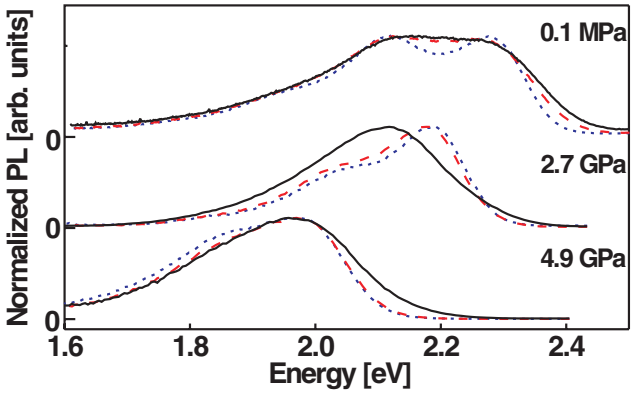

FIG. 4 (color online). Normalized PL spectra of a F8BT ($M_n = 112$ kDa) thin film at 0.1 MPa, 2.7 GPa, and 4.9 GPa for temperatures of 100 K (solid line), 230 K (dashed line), and 297 K (short-dashed line). The pressure variance over the temperature range was <0.5 GPa. The spectra were shifted vertically for clarity.

redshift of the time-resolved spectra is observed in the thin film than in the solid-state solution, as expected from the steady-state results presented in Fig. 1. We fit the PL decay of F8BT on the ns time scale for each of the conditions presented in Fig. 3. The PL decay of F8BT in solid-state solution at 0.1 MPa is monoexponential with a time constant of $\tau = 2.2$ ns across the visible spectrum. At 5.0 GPa, a faster monoexponential decay is observed, with a time constant of $\tau = 1.9$ ns. The faster decay rate may be correlated to the increased oscillator strength observed in absorption spectra at high pressures, a consequence of molecular planarization under pressure. The PL decay of the F8BT thin film at 0.1 MPa is monoexponential with a time constant of $\tau = 2.0$ ns. At 6.0 GPa, the PL decay of the thin film exhibits a dynamic redshift on the ns time scale. A global biexponential fit of the PL decay over the spectrum yields time constants of $\tau_1 = 0.6$ ns and $\tau_2 = 2.3$ ns. The longer-lived emission (τ_2) is dominant only at low energies and accounts for a small fraction (<0.05) of the total emission. The general influence of the external pressure is a faster PL decay rate, due in part to molecular planarization as evident in the solid-state solution. The greater change in the PL decay rate in thin films than in solid-state solutions suggests that closer intermolecular interaction allows for additional nonradiative decay channels under pressure.

In Fig. 4, temperature-dependent PL spectra of a F8BT thin film at 0.1 MPa, 2.7 GPa, and 4.9 GPa are presented. At 0.1 MPa, two emission peaks are clearly evident at 100 K. At higher temperatures, the contribution of the lower-energy emission increases, and thermal broadening is evident. At 2.7 GPa, a similar behavior is observed, redshifted with respect to the ambient pressure spectra. Donley *et al.* presented evidence for the existence of multiple emissive states in F8BT at 0.1 MPa as well as for energy transfer between these states [19]. The observation of two emission peaks at 100 K and 2.7 GPa suggests that at least two emissive states may be present at this intermediate pressure. At 4.9 GPa, one broad emission feature is observed at all temperatures, suggesting that a more significant change in the emissive states may occur at higher pressures.

In summary, we have demonstrated that both intra- and intermolecular pressure-induced effects significantly contribute to the observed redshift of the PL spectrum of F8BT at high pressure. We presented experimental and theoretical evidence for a reduction in the torsional angle, θ, between the F8 and BT subunits of F8BT at high pressure. In addition, time-resolved and temperature-dependent PL results suggest a limited role of direct intermolecular emission in thin films even at high external pressures.

The authors thank D. J. Dunstan, H. Hübel, and R. Beadle for assistance, and Cambridge Display Technology Ltd. for materials. This work was supported by the National Science Foundation Graduate Research Program and the Gates Cambridge Trust (J. P. S) with support from the Engineering and Physical Sciences Research Council (EPSRC). J. S. K. thanks the EPSRC for Grant No. RG38958.

*jpschmidtke@gmail.com

[1] J. H. Burroughes *et al.*, Nature (London) **347**, 539 (1990).
[2] H. Sirringhaus *et al.*, Science **280**, 1741 (1998).
[3] B. A. Gregg, J. Phys. Chem. B **107**, 4688 (2003).
[4] B. J. Schwartz, Annu. Rev. Phys. Chem. **54**, 141 (2003).
[5] J. L. Brédas *et al.*, Chem. Rev. **104**, 4971 (2004).
[6] L. M. Herz *et al.*, Chem. Phys. Lett. **347**, 318 (2001).
[7] J. Cornil *et al.*, J. Am. Chem. Soc. **120**, 1289 (1998).
[8] A. C. Morteani *et al.*, Adv. Mater. **15**, 1708 (2003).
[9] J. Mårdalen *et al.*, J. Phys. Condens. Matter **10**, 7145 (1998).
[10] S. Webster *et al.*, Polymer **37**, 4961 (1996).
[11] B. C. Hess *et al.*, Phys. Rev. Lett. **66**, 2364 (1991).
[12] S. Guha *et al.*, Phys. Rev. Lett. **82**, 3625 (1999).
[13] M. Hanfland *et al.*, J. Chem. Phys. **90**, 1930 (1989).
[14] M. A. Loi *et al.*, Phys. Rev. Lett. **86**, 732 (2001).
[15] B. C. Hess *et al.*, Phys. Rev. B **47**, 1407 (1993).
[16] C. M. Martin *et al.*, Phys. Rev. B **68**, 115203 (2003).
[17] R. K. Lammi *et al.*, Photochem. Photobiol. Sci. **4**, 95 (2005).
[18] J. K. Grey *et al.*, J. Phys. Chem. B **110**, 18898 (2006).
[19] C. L. Donley *et al.*, J. Am. Chem. Soc. **127**, 12890 (2005).
[20] J. S. Kim *et al.*, Adv. Mater. **14**, 206 (2002).
[21] M. Ariu *et al.*, Synth. Met. **111–112**, 607 (2000).
[22] G. Heimel *et al.*, Synth. Met. **116**, 163 (2001).
[23] Q. G. Zeng *et al.*, J. Lumin. **115**, 32 (2005).
[24] M. C. Zerner, in *Reviews in Computational Chemistry*, edited by K. Lipkowitz and D. B. Boyd (VCH, New York, 1994), Vol. 2, p. 313.
[25] M. J. Frisch *et al.*, computer code GAUSSIAN98, REV. A.11, 2001.
[26] W. F. Sherman, J. Phys. C **13**, 4601 (1980).
[27] E_{Abs} defined as the energy of 10% of the normalized absorption maximum.